

Absorption of Tar Content in Producer Gas using Used Cooking Oil in a Packed-bed Column

Firman Asto Putro^a, Joko Waluyo^b, Bahaul Fahmi Al Haq^b, Wahyu Nur Hidayat^b, Sunu Herwi Pranolo^{b,*}

^aChemical Engineering Diploma 3, Vocational School, Universitas Sebelas Maret, Surakarta, Indonesia 57126

^bChemical Engineering Department, Engineering Faculty, Universitas Sebelas Maret, Surakarta, Indonesia 57126

*Corresponding author: sunu_pranolo@staff.uns.ac.id

DOI: <https://dx.doi.org/10.20961/equilibrium.v7i1.70383>

Article History

Received: 13-01-2023, Accepted: 06-03-2023, Published: 10-03-2023

Keywords:
producer gas, mass transfer coefficient, packed-bed column, tar, used-cooking oil

ABSTRACT. The tar content in producer gas may cause crusting on the engine if it is utilized as a fuel gas, thus it needs to be removed. This study aims to determine the liquid phase mass transfer coefficient in removing tar from producer gas in a packed-bed contactor column. This process is carried out continuously using used-cooking oil as an absorbent. This was carried out by contacting the producer gas as a product of cocoa pod-husk gasification at the temperature range of 491-940°C at a certain counter-current flow rate with used-cooking oil in a column with a Raschig ring packing bed. The study used packed-bed materials with specific surface areas of 29.3927 m²/m³, 49.7532 m²/m³, 95.4113 m²/m³, 96.8182 m²/m³, 101.6840 m²/m³, and 105.0128 m²/m³, and with the linear velocity of used-cooking oil ranging from 0.0229 m/s to 0.0827 m/s. A mass transfer coefficient mathematical model has been constructed based on the research results. The model applies to the ranges (As.dt), (D_L/dt.v_L), and (μ_L / ρ_L.v_L.dt) from 2.2397 to 8.0020, 2.26.10-10 to 1.72.10-9, and 0.0331 to 0.3102, respectively, with an average error of 9.33%. The average tar removed was 87%.

1. INTRODUCTION

Energy consumption always increases from time to time. In 2015, the national final energy requirement was 5.393 million TJ, and it is estimated that by 2025 it will increase 1.8 times with an average growth rate of 6.4%. Energy needs that always increase are not followed by an increase the energy source itself. As a result, conventional energy sources continue to decrease from day to day. Various efforts continue to be made to meet these energy needs. New renewable energy sources are very promising solutions. One of these renewable sources is biomass. In 2017, energy production from biomass was 0.4 million TJ. Utilizing biomass energy with the gasification method is the most flexible because the producer gas produced can be used directly as a fuel gas or as a fuel for engines. Besides that it can also be used as a raw material for the chemical industry. However, various problems arise that must be resolved when developing gasification as an alternative energy source. One of them is the tar content in producer gas (gasification gas).

The gas produced by the gasification of biomass contains several impurities: namely dust, unburned residues, soot, water vapor, and tar (heavy hydrocarbon mixtures). Tar is condensed in a temperature range of 180-300°C, and when it condenses, it becomes a sticky liquid, and together with the dust, it forms a deposit that is difficult to remove [1]. The type of gasifier determines the tar content of the gasification producer gas. According to [2] the tar contents of updrafts, fluid beds, and downdraft gasifiers are 100 g/Nm³, 10 g/Nm³, and 1 g/Nm³, respectively. While the tar content for internal combustion machine operations is less than 0.1 g/Nm³. Thus, we need cleaning technology to use gas producers.

Some research has been carried out to develop techniques such as catalytic cracking, thermal cracking, scrubbing technology, or using plasma reactors to remove tar effectively, but most are not cheap enough for gasification applications in rural power plants. The selection of tar removal techniques is based on the location where the tar will be removed. In the primary method, tar is removed in the gasification reactor. While in the second method, tar is removed by installing a gas cleaning unit outside the reactor; this is more efficient, economical, and easier to regulate. Besides that, it can also be done with chemical treatment (catalytic cracking and thermal cracking) and physical treatment (adsorption and absorption). The physical process is more interesting because technically and economically it is more profitable and it is not difficult to apply it in various gasification

systems. Physical treatment can be divided into wet systems (spray tower and packed column scrubber) and dry systems (cyclone, filters, and adsorption) [3].

Research on tar separation using the dry system method has been carried out by M. Awais et al, 2018 [4] who used a cyclone to separate tar from gas produced from the gasification of wood with a length and width of 2.5-3.5 cm with a thickness of 1.6-2.6 cm and corn cobs with a length and width of 7.0-8.0 cm with a thickness of 3.6-5.0 cm. Using downdraft gasifier, they successfully reduced the tar content from 6600-7500 mg/m³ to 1827-2582 mg/m³ or 66%-72%. Nakamura et al., (2016) used activated carbon filters with an updraft gasifier to separate tar from Japanese cedar gasification (*Cryptomeria japonica*). They succeeded in reducing tar levels from 2.53 g/m³ to 0.47 g/m³ or 81.5%. As for R. Cimerman et al, 2017 [5] they used the Non-Thermal Plasma Method with TiO₂ catalyst to remove tar with the Naphthalene tar model and successfully eliminated 80% of the tar.

On an industrial scale, the wet system method does not only focus on the type of absorbent used but also on the concept of the scrubber design. The Güssing Plant in Austria removes benzene and tar from the downdraft gasifier using a rapeseed-methyl-ester (RME) scrubber at 5°C [6]. OLGA technology developed by the Energy Research Center of the Netherlands uses a special oil scrubber tower to regenerate oil using water or steam for de-absorption of 99% heavy and light tar from a bubbling fluidized bed (BFB) and for the experiments on tar phenol models [7].

Several investigators have conducted previous studies of tar removal by absorption method. The studies have been performed using gravimetric calculations to assess the effectiveness of tar removal, considering several parameters such as the type of absorbent, equipment configuration, operating conditions, and type of feedstock. A. Paethanom et al, 2012 [3] managed to trap 95.4% of tar derived from rice husk pyrolysis, which was set at 800°C and vegetable oil as the absorbent. S. Nakamura et al., 2016 [8] used vegetable oil bubble and packed-bed scrubbers in combination with an adsorbent char to separate tar from the gasification of Japanese cedar (*Cryptomeria japonica*), yielding a tar reduction of 98%. Whereas, T. Phuphuakrat et al., 2011 [9] managed to remove 60.4% of the tar derived from a pyrolizer reactor with 0.71-1.00 mm wood chip bait (*Jacendar panese*) fed at 0.6 g/min and with nitrogen as a carrier gas at 1.5 L/minute by using vegetable oil in the bubble scrubber. There is also S. Unyaphan et al., 2016 [10], who used 7.5% emulsified vegetable oil on a bubble scrubber and successfully removed 87.6% of the tar from the 800°C pyrolizer reactor with 0.5-1.0 mm Japanese cedar bait at 0.6 g/minute with nitrogen as a carrier gas at 0.8 L/minute. In the following year, S. Unyaphan et al., 2017 [11] used canola oil in the venturi scrubber to absorb tar from a fixed bed pyrolizer reactor at a temperature of 800°C with 0.5-1.0 mm Japanese cedar fed at 0.6 g/minute and nitrogen as gas at 0.8 L/minute as a carrier for laboratory scale experiments. For commercial scale, they used an 800°C bubbling fluidized bed gasifier (BFBG) with rice husks fed at 260 kg/hour and air at 375 Nm³/hour as the gasifier agent, resulting in ratio of 0.35; they succeeded in reducing tar content by 90% - 96%. The spray tower used a water absorber to remove sludge-derived tar from the product gas via a downdraft gasifier, successfully removing 39% of the tar[12]. The present study evaluated the tar removal performance of cocoa pod-husk gasification with a used cooking oil scrubber by numerical approach. a

The previous studies evaluated tar removal performance by trial and error with varying parameters like type of absorbent, equipment configuration, and operating conditions. To optimize the absorption process, the present study developed a mass transfer coefficient mathematical model by numerical approach. The parameters involved in this study are absorbent flowrate and packing surface area. This study aims to construct model models that apply to a certain range of operating conditions.

2. MATERIALS AND METHODS

2.1 Model development

2.1.1 Mass transfer

Gas producers with tar $C_{Ag}|_z$ enter through an absorber at height z and exit at $z + \Delta z$ with levels $C_{Ag}|_{z+\Delta z}$ in contact with UCO in a counter-current mode on a volume element filled with packed-bed material, such as shown in Fig. 1. The tar mass in the gas phase (producer gas) moves into the liquid phase (UCO) through the resistance of the gas phase film and liquid phase. In this study, it is assumed that resistances are only in the liquid phase, so the concentration of tar in the gas body is the same as that on the border between phases. The qualitative tar concentration profile is shown in Fig. 2.

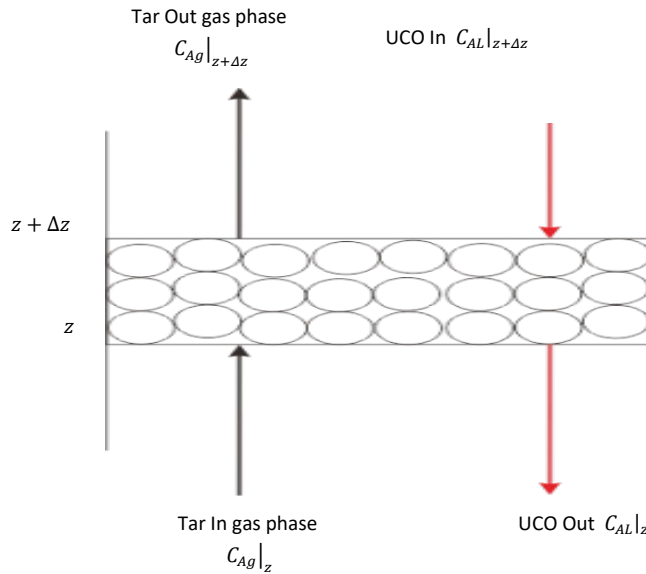


Figure 1. Review of Element Volume

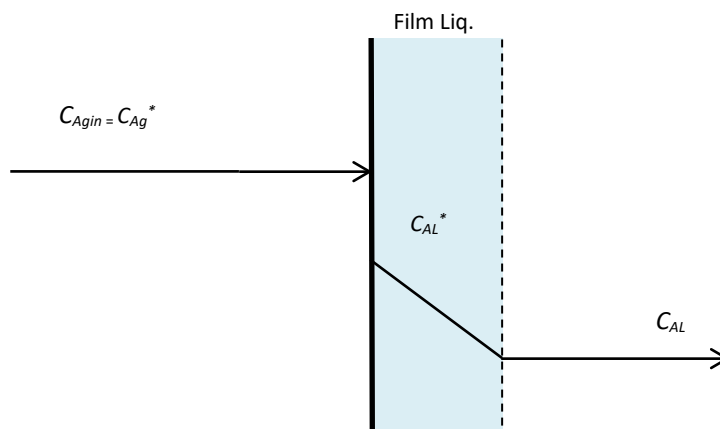


Figure 2. Tar Mass Transfer Scheme from the Gas Phase to the Liquid Phase, Assuming that Obstacles are Only in the Liquid Phase

The balance of the tar mass in phase on a volume element as thick as Δz follows: *Rate of input tar mass - rate of mass of output tar - mass rate of tar transferred to liquid = the rate of mass accumulation of tar*. In the state of steady state, the mass accumulation rate of tar = 0, then:

$$V_g \cdot C_{Ag}|_z - V_g \cdot C_{Ag}|_{z+\Delta z} - N_A A = 0 \quad (1)$$

where V_g is the gas flow rate (cm^3/s), C_{Ag} is the concentration of tar in gas (mg/cm^3), the area of mass transfer area (cm^2), and N_A is the flux transfer of the mass of tar into UCO ($\text{mg}/(\text{cm}^2 \cdot \text{s})$). Based on Fig. 2, it is assumed that the barriers to mass transfer are only found in the liquid film strip. Then the following equation applies:

$$N_A = -k_L \cdot (C_{AL} - C_{AL}^*) \quad (2)$$

where k_L is the mass transfer constant in the liquid, C_{AL} is the concentration of tar in liquid, and C_{AL}^* is the concentration of tar in the liquid which is equilibrium with the concentration of tar in the gas (C_{Ag}). The relationship between C_{Ag} and C_{AL}^* is shown in Equation 3.

$$C_{Ag} = H \cdot C_{AL}^* \quad (3)$$

the following equation is obtained:

$$V_g \cdot C_{Ag}|_z - V_g \cdot C_{Ag}|_{z+\Delta z} - (-k_L \cdot (C_{AL} - C_{AL}^*)) \cdot A = 0$$

$$V_g \cdot C_{Ag}|_z - V_g \cdot C_{Ag}|_{z+\Delta z} + k_L \cdot A \cdot (C_{AL} - C_{AL}^*) = 0$$

Because it will be difficult to measure the surface area of the mass transfer field (A) directly, it is assumed that the liquid only moistens the surface of the packing so that the area of mass transfer is equal to the surface area of the filling and k_L multiplied by parameter a . So, the following equation applies:

$$k_L a = k_L \cdot \frac{A}{V} \quad (4)$$

where parameter a is the area of mass transfer unity volume of mass transfer equipment. So, the following equation is obtained:

$$V_g \cdot C_{Ag}|_z - V_g \cdot C_{Ag}|_{z+\Delta z} + k_L a \cdot V \cdot (C_{AL} - C_{AL}^*) = 0$$

where V is the volume of mass transfer equipment and the following is obtained.

$$V_g C_{Ag}|_z - V_g C_{Ag}|_{z+\Delta z} + k_L a \cdot A_t \cdot \Delta z \cdot (C_{AL} - C_{AL}^*) = 0$$

$$V_g \cdot C_{Ag}|_{z+\Delta z} - V_g \cdot C_{Ag}|_z = k_L a \cdot A_t \cdot \Delta z \cdot (C_{AL} - C_{AL}^*)$$

Both segments are divided by Δz and wrapped in $\Delta z \rightarrow 0$:

$$\lim_{\Delta z \rightarrow 0} \frac{V_g \cdot (C_{Ag}|_{z+\Delta z} - C_{Ag}|_z)}{\Delta z} = k_L a \cdot A_t \cdot (C_{AL} - C_{AL}^*)$$

$$V_g \cdot \frac{dC_{Ag}}{dz} = k_L a \cdot A_t \cdot (C_{AL} - C_{AL}^*)$$

$$V_g \cdot \int dC_{Ag} = k_L a \cdot A_t \cdot \int (C_{AL} - C_{AL}^*) dz$$

$$V_g \cdot (C_{Agin} - C_{Agout}) = k_L a \cdot A_t \cdot (C_{AL} - C_{AL}^*) \cdot \Delta z$$

thus,

$$k_L a = \frac{V_g \cdot (C_{Agin} - C_{Agout})}{A_t \cdot \Delta z \cdot (C_{AL} - C_{AL}^*)} \quad (5)$$

2.1.2 Analysis of Dimensional Numbers

The relationship between experimental variables with $k_L a$ (1/s) is modeled in the form of dimensionless equations. Dimensional equations do not depend on the geometry scale, so they can be used for scale-up purposes. Dimension analysis is solved by the Buckingham method. The variables influence the price of $k_L a$ in the absorption process, namely: specific surface area (A_s , m²/m³), column diameter (d_t , m), UCO diffusivity (D_L , m²/s), UCO density (ρ_L , kg/m³), UCO viscosity (μ_L , kg/m.s), and UCO linear velocity (v_L , m/s). The relationship between the above variables is expressed by the following equation:

$$k_L a = f(A_s, d_t, D_L, v_L, \mu_L, \rho_L) \quad (6)$$

Completion with the Buckingham method gives the following:

$$\frac{k_L a \cdot d_t}{v_L} = K \cdot (A_s \cdot d_t)^a \cdot \left(\frac{D_L}{d_t \cdot v_L}\right)^b \cdot \left(\frac{\mu_L}{\rho_L \cdot v_L \cdot d_t}\right)^c \quad (7)$$

The constant values K , a , b , and c are evaluated by multivariable linear regression methods, so that the empirical equation $k_L a$ is obtained.

2.2 Materials and Tools

The material used in this study is used cooking oil (UCO) obtained from restaurant businesses in Klaten city area and around the city of Solo. Filtration was done to remove the solid particles contained in the oil. Gas was produced from cocoa pod-husk gassification at temperature range of 410 – 490°C.. The physical properties of UCO and the specifications of the packing material used are presented in Table 1. The absorber used was 7.62 cm in diameter with a total height of 45 cm, and it was filled with 3 stages with a height of 15 cm each. The scheme of the experimental device used for the absorption of tar using UCO is shown in Fig. 3.

Table 1. UCO and packing specifications

i – th experiment	Packing type	ρ_L , kg/m ³	$\mu_L \times 10^5$ kg/m.s	ε	Ψ	A_s (m ² /m ³)
1	Sphere 1	0.3156	4.33	0.8040	1	29.393
2	Sphere 2	0.3365	4.00	0.7927	1	49.753
3	Sphere 3	0.3207	4.09	0.7614	1	95.411
4	Raschig ring 1	0.3447	3.99	0.9809	0.17	96.818
5	Raschig ring 2	0.3014	3.98	0.9801	0.14	101.684
6	Raschig ring 3	0.2940	4.31	0.9800	0.12	105.013

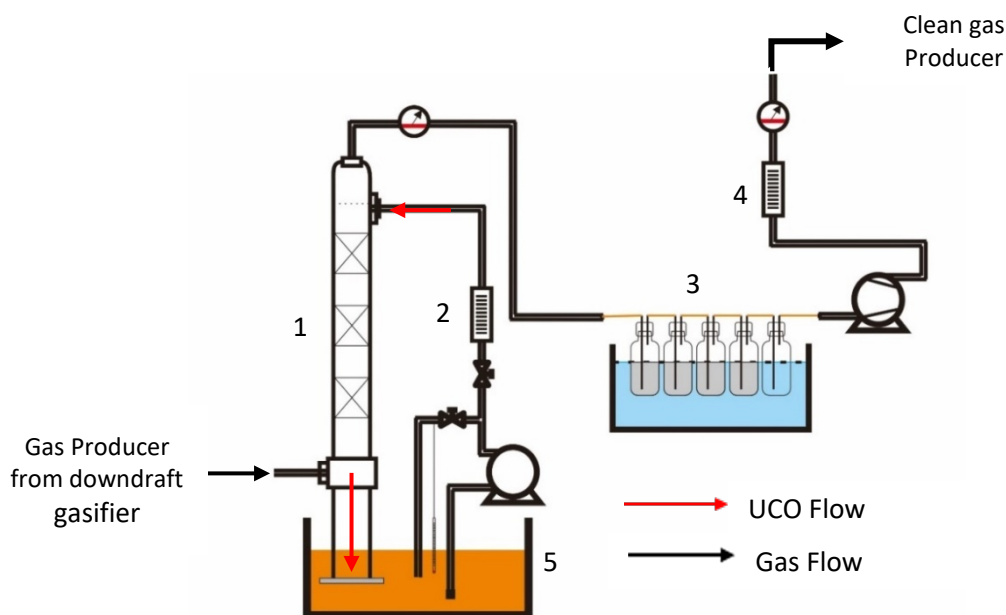


Figure 3. Scheme of Tar Absorption Research Set, (1) Packed-bed Column, (2) Rotameter UCO, (3) Impinger, (4) Rotameter Gas Producer, (5) UCO Tank

2.3 Test Method

The research work was divided into three stages, namely: Material Preparation, Data Collection, and Results Testing. Material preparation includes filtering UCO with gauze and igniting the gasifier with a feed flow rate of 0.1 kg/min and an air flow rate 126 L/min. Data retrieval includes the measurement of the UCO volumetric flow rate into the absorber with a rotameter, measurement of the volumetric gas producer flow rate with rotameter, and taking the sample with an impinger.. The results of the test include analysing the tar content in the producer gas by the gravimetric method and the UCO viscosity by the falling sphere method; the UCO density was measured by weighing in a pycnometer.

2.4 DATA PROCESSING

THE DATA OBTAINED WERE USED TO CALCULATE THE VALUE OF K_{LA} BASED ON MASS BALANCE RE-VIEW USING EQUATION (5), THEN K_{LA} WAS OBTAINED AND EXPERIMENTAL

DATA WAS USED TO FIND THE PARAMETERS OF EMPIRICAL EQUATIONS OF GROUPS OF DIMENSIONLESS NUMBERS IN EQUATION (7).

3. RESULTS AND DISCUSSION

Research on tar absorption using packed bed columns has been carried out with variations in absorbent flow rates and specific surface areas of packing beds. The results of the experimental mass transfer coefficients and models are presented in Fig. 4. In this study, the factors that influence the value of the liquid phase transfer coefficient of the tar into the UCO include the specific surface area of the packing bed, the form of the packing bed, and the absorbent flow rate.

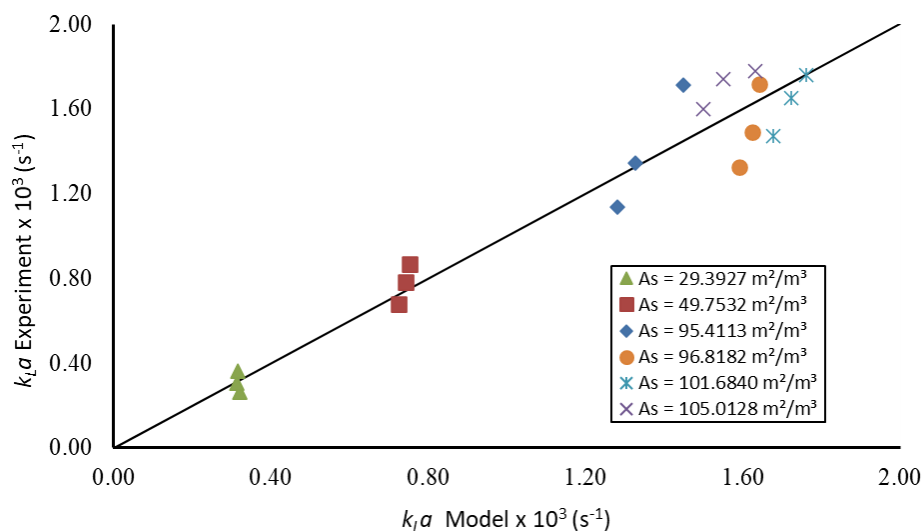


Figure 4. $k_L a$ Experiments and $k_L a$ Models

3.1 Packing Surface Area

Variation of the specific surface area of the packing bed was carried out to determine its effect on the liquid phase mass transfer coefficient of tar into the UCO. Table 1 presents the results of the trial results on variations in the specific surface area of the packing bed. The largest $k_L a$ value was obtained on the specific surface area of the fillings $105.0128 \text{ m}^2/\text{m}^3$ and the linear flow rate of UCO $5.24 \times 10^{-5} \text{ m}^3/\text{s}$ is $1.78 \times 10^{-3}/\text{s}$. The effect of A_s on $k_L a$ based on variations in UCO flow rate is shown in Fig. 5.

The experiments used sphere and Raschig ring packing beds treated with variations in the flow rates of $3.18 \times 10^{-5} \text{ m}^3/\text{s}$, $4.24 \times 10^{-5} \text{ m}^3/\text{s}$, and $5.30 \times 10^{-5} \text{ m}^3/\text{s}$. The highest $k_L a$ obtained on the specific surface area of the packing bed was $105.0128 \text{ m}^2/\text{m}^3$. From the results of this experiment, it can be concluded that the specific surface area of the packing bed (A_s) has a positive effect on increasing the liquid phase mass transfer coefficient ($k_L a$).

S.H Pranolo et al, 2018 [13] conducted experiments to determine the transfer coefficient of the liquid phase mass of H_2S gas from biogas into the digester effluent using a column of packing bed. For variations in the biogas flow rate in the range of $0.1109\text{-}0.8846 \text{ m}^3/\text{hour}$ and the contact surface area of the packing bed in the range of $0.2992\text{-}0.9269 \text{ m}^2/\text{m}^3$, they obtained the largest $k_L a$ value with the contact surface area of $0.6279 \text{ m}^2/\text{m}^3$ and a biogas flow rate $0.000183 \text{ m}^3/\text{hour}$, which is $0.0113/\text{s}$. According to the experiment, that the specific surface area gives a straight line against $k_L a$.

Habaki et al, 2007 [14] compared the effect of the type of Pall Ring and Super Mini Ring (SMR) type on CO_2 gas absorption using mono-ethanolamine (MEA) solution. Each packing has a total surface area of $360 \text{ m}^2/\text{m}^3$ and $420 \text{ m}^2/\text{m}^3$, respectively. Super Mini Ring (SMR) provides a higher absorption performance than Pall Ring because it has a smaller pressure drop and a larger surface area. This is in accordance with mass transfer theory, the mass transfer coefficient is proportional to the contact surface area.

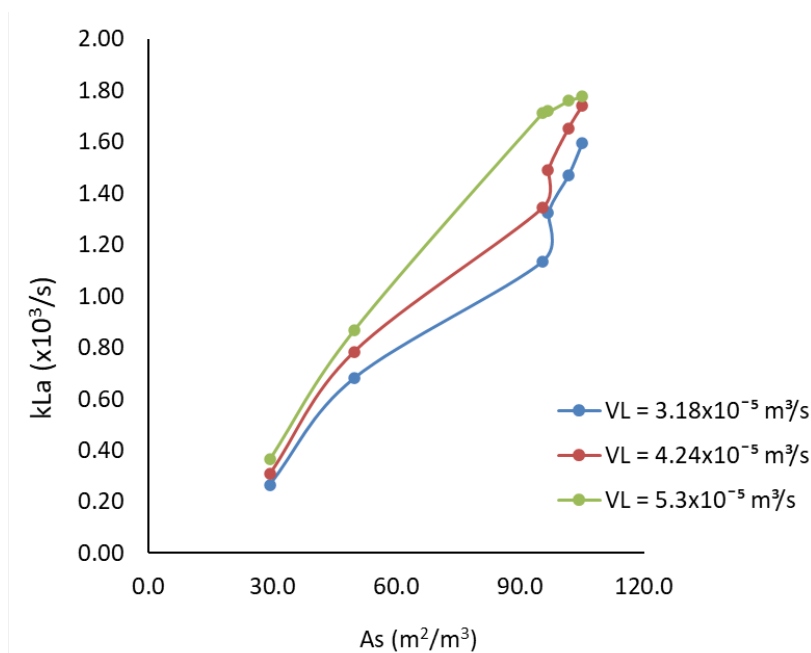


Figure 5. Effect of Specific Surface Area of Packing (A_s) on $k_L a$

3.2 Sphericity Of Packing

This study uses two types of packing, namely spheres and Raschig rings. The characteristics of each ingredient are presented in Table 1. The form factor of sphericity consists of 4 variations, namely 0.12, 0.14, 0.17, and 1. The $k_L a$ value for spherical fillings is always smaller than for a Raschig ring packing bed. The value of $k_L a$ for the same type of material is influenced by the contact surface area. For a spherical type packing bed that has a form factor, sphericity ($\Psi = 1$), the value of $k_L a$ is very dependent on the area of contact surface. Piping type material that has smaller sphericity will have a larger contact area so that the obtained $k_L a$ value is greater. This is consistent with the research conducted by [15].

G.H Sedahmed et al, 2013 [15] compared the effect of the shape and size of packing beds (Raschig ring, cylinder, and sphere), superficial speed of gas and liquid, and physical properties of the solution. A range of factors increased mass and heat transfer speeds from 1.1 to 6.1. For one-phase fluid flow, the factors for increasing mass transfer and successive heat were in the order of Raschig ring > cylinder > sphere. Thus, it can be concluded that the form factor of sphericity is inversely proportional to the value of the liquid phase mass transfer coefficient.

3.3 Absorbent linear flow rate

In the same type of packing, increasing the flow rate of UCO (V_L) will increase the linear flow of UCO (v_L). The effect of v_L linear flow rate on $k_L a$ based on variations in the specific surface area of the packing bed is shown in Fig. 6. Fig. 6 presents the $k_L a$ value for various types of packing beds. Stuffing material has a specific surface area of 29.3927 m²/m³, 49.7532 m²/m³, 95.4113 m²/m³, 96.8182 m²/m³, 101.6840 m²/m³, and 105.0128 m²/m³. The highest $k_L a$ obtained for each packing bed is treated with a flow rate of UCO 4.0×10^{-2} m/s. Of all the curves in Fig. 6, the type of Raschig ring 3 packing bed that has the largest specific surface area compared to other types of packing beds turns out to produce the largest mass transfer coefficient value, which is $1,78 \times 10^{-3}$ /s. From the results of this experiment, it can be concluded that the flow rate of UCO (v_L) has a positive effect on the increase in the liquid phase mass transfer coefficient ($k_L a$). This is consistent with the research of [16] and [17].

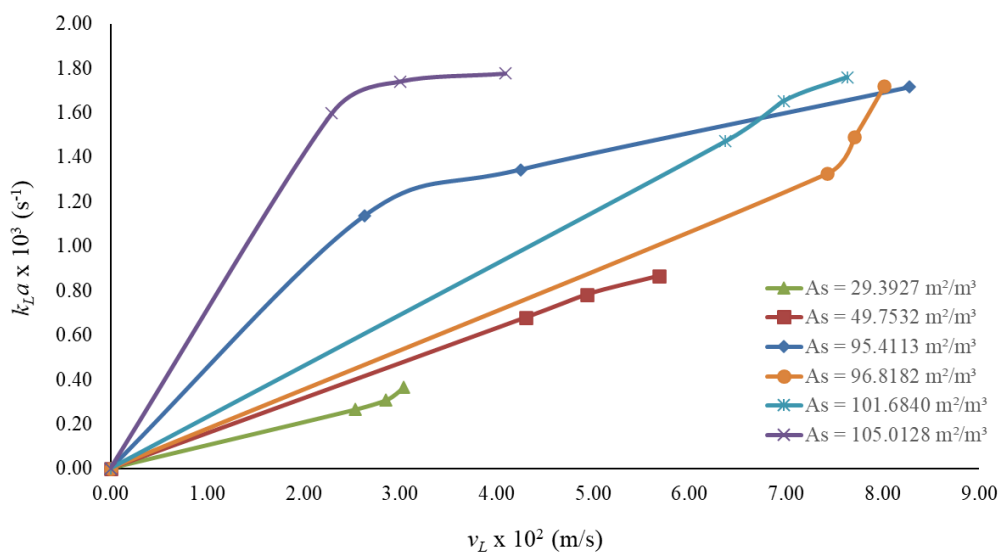


Figure 6. Effect of Linier UCO Flow Rate (v_L) on $k_L a$

M. Hanif et al, 2012 [16] conducted a study of the effect of gas and liquid flow rates on the rate of CO₂ and H₂O absorption in a packed column. They concluded that the effect of the gas flow rate and flow rate of the liquid were directly proportional to the value of $k_L a$. T. Welasih, 2006 [17] conducted an experiment to determine the moving coefficient value of the liquid-solid mass in the column containing the adsorption method. This research used local activated carbon as its adsorbent and benzoic acid solution as its absorbate; the packed bed column was 6.3 cm in diameter and 40 cm in height. The conclusion was the same as [16]; the price of the mass transfer coefficient ($k_L a$) is greater with increasing the speed of liquid flow at the initial fixed concentration. In his research, the price of $k_L a$ was 0.03287-0.03390/s at the fluid flow rate of 10-30 mL/s and the initial concentration was 0.01-0.03 mol/L.

In Fig. 6, with the same type of packing bed or specific surface area increases, $k_L a$ tends to be insignificant when the UCO linear flow rate increases. This is consistent with the empirical equation obtained (Equation 8) where $k_L a \sim v_L^{0.1026}$, and similar results were obtained by P.R. Bhoi et al, 2015 [18] when conducting tar adsorption model studies in which benzene, toluene, and ethylbenzene were used as tar and canola oil was solvent on packed-bed column. It was found that there was not a significant increase in the efficiency of tar reduction which resulted in a significant increase in the price of $k_L a$.

3.4 Tar Reduction

In this study, the tar reduction was obtained from various packing beds, as shown in Fig 7. The average tar concentration in producer gas coming out gasifier is approximately at 0.00825 kg/m³. The highest tar reduction is around 93%-94% at the UCO linear flow rate of 2.3×10^{-2} m/s up to 4.1×10^{-2} m/s with the largest A_s at 105.013 m²/m³, and the lowest is around 65%-72% in the 2.5×10^{-2} m/s up to 3.0×10^{-2} m/s with the smallest A_s 29,393 m²/m³. In the same type of packing bed, tar reduction tends to increase as the linear flow rate increases from UCO. The effect of increasing v_L on the tar reduction tends to be insignificant in the tar reduction. Something similar was also obtained by [18] and [19].

P.R. Bhoi et al, 2015 [18] conducted tar adsorption with canola oil as a solvent on the packed-bed scrubber with a range of solvent flow rates from 53–73 mL/min. The value of tar reduction was relatively stable at 90%-97%. Similarly, A.G. Bhave et al, 2008 [19] who carried out gas cleaning from gas and biomass gasification from tar and dust, used a combination of packed bed scrubbers and water and sand filter solvents. When the variation of producer gas flow rate was carried out between 49-56 m³/hr at the solvent flow rate (370 L/hr) the cleaning efficiency was around 70%-90%. The average value of tar reduction in this study is 87%. The value is in the range of the tar removal, 60.4%-98%, using organic solvents [3, 8-11, 18].

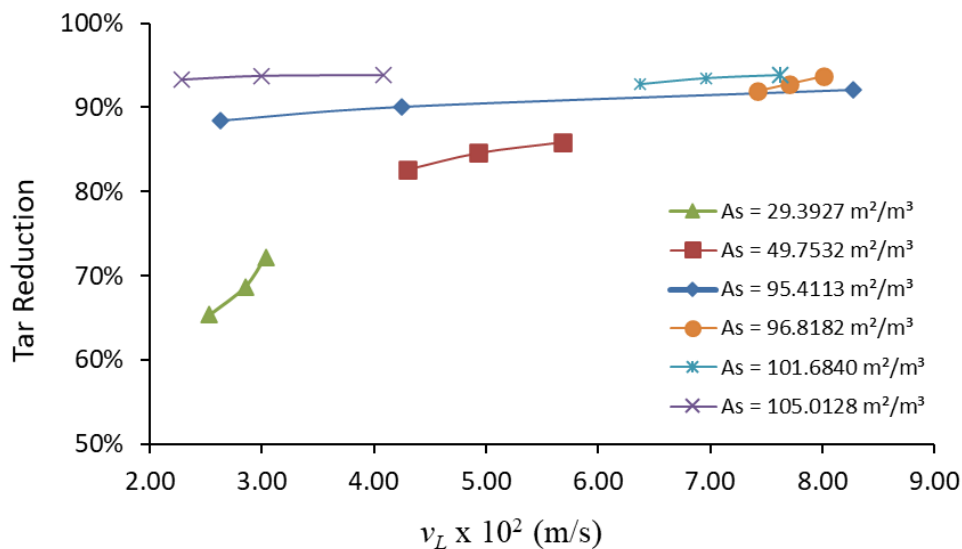


Figure 7. Effect of the UCO Linear Flow Rate on Tar Reduction at different Types of Packing

3.5 Empirical Equations of The Coefficient of Mass Transfer

Mathematically, the following equation shows the relationship between the liquid phase mass transfer coefficient and the factors that influence it:

$$k_L a \cdot \frac{d_t}{v_L} = 29,0530 \cdot [A_s \cdot d_t]^{1,2776} \cdot \left[\frac{D_L}{d_t \cdot v_L} \right]^{0,5257} \cdot \left[\frac{\mu_L}{\rho_L \cdot v_L \cdot d_t} \right]^{0,3665}$$

The dimensionless equation shows the correlation between the UCO linear velocity and the specific surface area of the packing bed. The linear velocity of UCO and the specific surface area of the packing bed are directly proportional to $k_L a$. The equation applies to ranges of $(A_s \cdot d_t)$, $(D_L/d_t \cdot v_L)$, and $(\mu_L/\rho_L \cdot v_L \cdot d_t)$ from 2.2397 to 8.0020, from $2.26 \cdot 10^{-10}$ to $1,72 \cdot 10^{-9}$, and from 0.0331 to 0.3102, respectively, with an average error of 9.33%.

4. CONCLUSION

Research shows the relationship between the variables studied and mass transfer coefficients. It can be concluded that the specific surface area of the packing bed (A_s) and the linear flow rate of UCO (v_L) are positively proportional to the liquid phase mass transfer coefficient ($k_L a \sim A_s^{1,3352}$, $k_L a \sim v_L^{0,1026}$). The equation applies to the range of $(A_s \cdot d_t)$, $(D_L/d_t \cdot v_L)$, and $(\mu_L/\rho_L \cdot v_L \cdot d_t)$ from 2.2397 to 8.0020, 2.26×10^{-10} up to 1.72×10^{-9} , and from 0.0331 to 0.3102, respectively, with an average error of 9.33%. The form factor of sphericity is positively proportional to the value of the liquid phase mass transfer coefficient, where the material for the type of Raschig ring sphericity is negatively related to the specific surface area of the packing bed (A_s). At the same sphericity, the value of the liquid phase mass transfer coefficient affected by the value of A_s . The average success of tar reduction is 87%, with package area parameters having the greatest impact.

ACKNOWLEDGEMENTS

The author would like to thank the Sebelas Maret LPPM University through the Fundamental Research Program of Sebelas Maret University's PNBFP Funds for Fiscal Year 2018 Number: 543/ UN27.21/PP/ 2018 which financed this research. Also, thank you to the Tani Makmur farmer group in Jumapolo, Karanganyar who provided cocoa fruit skin and to Janti Fishing in Klaten, food stalls Jepun, and other food stalls around Universitas Sebelas Maret that have provided UCO in this study.

NOTATION

μ_L	Viscosity UCO, $kg/(m.s)$
A	Area of mass transfer, m^2
a	Area of mass transfer area per unit volume of mass transfer equipment, m^2/m^3
A_s	Specific surface area, m^2/m^3
A_t	Cross section area of equipment, m^2
C_{Ag}	Concentration of tar in gas, kg/m^3
C_{AL}	Concentration of tar in liquid, kg/m^3
C_{AL}^*	Concentration of tar in an equilibrium liquid with Concentration of tar in gas, kg/m^3
D_L	Diffusivities UCO, m^2/s
D_t	Diameter of column, m
H	Henry's Constant
$k_L a$	Constant phase liquid transfer constant, $1/s$
N_A	Flux transfers tar mass into UCO, $kg/(m^2.s)$
V	Volume of mass transfer equipment, m^3
v_L	UCO linear flow rate, m/s
V_L	Flow rate of UCO, m^3/s
ε	Void fraction
ρ_L	Density of UCO, kg/m^3
Ψ	Sphericity

REFERENCES

- [1] M. Balas, M. Lisy, Z. Skala, J. Pospisil, Wet scrubber for cleaning of syngas from biomass gasification, *Advances in Environmental Sciences, Development and Chemistry* (2016).
- [2] T.A. Milne, R.J. Evans, N. Abatzoglou, Biomass Gasifier “Tars”: Their Nature, Formation, and Conversion, *National Renewable Energy Laboratory* (1998).
- [3] A. Paethanom, S. Nakahara, M. Kobayashi, P. Prawisudha, K. Yoshikawa, Performance of tar removal by absorption and adsorption for biomass gasification, *Fuel Processing Technology* 104 (2012) 144-154.
- [4] M. Awais, W. Li, A. Arshad, Z. Haydar, N. Yaqoob, S. Hussain, Evaluating removal of tar contents in syngas produced from downdraft biomass gasification system, *International Journal of Green Energy* 15(12) (2018) 724-731.
- [5] R. Cimerman, D. Račková, H. K., Tar Removal by Combination of Plasma with Catalyst WDS'17 *Proceedings of Contributed Papers - Physics* 127 (2017) 127-132.
- [6] R.W.R. Zwart, Gas cleaning downstream biomass gasification, *Status report 2009* (2009).
- [7] P.C.A. Bergman, S.V.B. Van Paasen, H. Boerrigter, The novel 'OLGA' technology for complete tar removal from biomass producer gas, (2002).
- [8] S. Nakamura, S. Kitano, K. Yoshikawa, Biomass gasification process with the tar removal technologies utilizing bio-oil scrubber and char bed, *Applied Energy* 170 (2016) 186-192.
- [9] T. Phuphuakrat, T. Namioka, K. Yoshikawa, Absorptive removal of biomass tar using water and oily materials, *Bioresour Technol* 102(2) (2011) 543-9.
- [10] S. Unyaphan, T. Tarnpradab, F. Takahashi, K. Yoshikawa, Effect of emulsified absorbent for tar removal in biomass gasification process, *Biofuels* 7(3) (2016) 233-243.
- [11] S. Unyaphan, T. Tarnpradab, F. Takahashi, K. Yoshikawa, Improvement of tar removal performance of oil scrubber by producing syngas microbubbles, *Applied Energy* 205 (2017) 802-812.
- [12] M. Dogru, A. Midilli, C.R. Howarth, Gasification of sewage sludge using a throated downdraft gasifier and uncertainty analysis, *Fuel Processing Technology* 75 (2002) 55-82.
- [13] S.H. Pranolo, Paryanto., Margono., B. Rizaldy, H. Yansah, Hydrogen Sulfide Removal from Biogas Using Digester Effluent Absorbent in a Continuous Vertical Column Reaktor 18 (2018) 160-165.
- [14] H. Habaki, J.M. Perera, S.E. Kentish, G.W. Stevens, W. Fei, CO₂Absorption Behavior with a Novel Random Packing: Super Mini Ring, *Separation Science and Technology* 42(4) (2007) 701-716.

- [15] G.H. Sedahmed, Y.A. El-Taweel, A.H. Konsowa, M.H. Abdel-Aziz, Effect of packing geometry on the rate of mass and heat transfer at a vertical tube imbedded in fixed bed under single and two phase flow, *International Communications in Heat and Mass Transfer* 48 (2013) 149-154.
- [16] M. Hanif, M.H. Al Rasid, Pengaruh Laju Alir Gas dan Cairan pada Absorpsi Gas CO₂ oleh H₂O dalam Packed Column, *Prosiding SNSMAIP III* (2012) 459-463.
- [17] T. Welasih, Penentuan Koefisien Perpindahan Massa Liquid Solid dalam Kolom Packed Bed dengan Metode Adsorpsi, *Jurnal Teknik Kimia* 1 (2006).
- [18] P.R. Bhoi, R.L. Huhnke, A. Kumar, M.E. Payton, K.N. Patil, J.R. Whiteley, Vegetable oil as a solvent for removing producer gas tar compounds, *Fuel Processing Technology* 133 (2015) 97-104.
- [19] A.G. Bhave, D.K. Vyas, J.B. Patel, A wet packed bed scrubber-based producer gas cooling–cleaning system, *Renewable Energy* 33(7) (2008) 1716-1720.